

RESEARCH ARTICLE | JULY 23 2025

Traveling wave on a phase-segregated metal composite caused by electrochemical reaction: Direct monitoring for silver-wave

Yuko Nagamine   ; Kenichi Yoshikawa 



AIP Advances 15, 075040 (2025)

<https://doi.org/10.1063/5.0259604>



Special Topics Open for Submissions

[Learn More](#)

Traveling wave on a phase-segregated metal composite caused by electrochemical reaction: Direct monitoring for silver-wave

Cite as: AIP Advances 15, 075040 (2025); doi: 10.1063/5.0259604

Submitted: 20 January 2025 • Accepted: 11 July 2025 •

Published Online: 23 July 2025



View Online



Export Citation



CrossMark

Yuko Nagamine^{1,a)}  and Kenichi Yoshikawa² 

AFFILIATIONS

¹ Department of Intelligent System Engineering, National Institute of Technology, Ube College, Ube, Yamaguchi 755-8555, Japan

² Faculty of Life and Medical Sciences, Doshisha University, Kyotanabe, Kyoto 610-0321, Japan

^{a)} Author to whom correspondence should be addressed: ynagamin@ube-k.ac.jp. Tel./Fax: +81-836-35-4993

ABSTRACT

Here, spatiotemporal pattern formation on the electrode surface in an electrochemical system was studied. We performed an experiment for dynamic pattern formation accompanied by Ag and Sb co-electrodeposition through real-time visual inspection, together with *in situ* elemental analysis. The time evolution of the Ag-rich domain as a chemical wave was successfully monitored using x-ray visualization. The results indicate that the occurrence of a traveling wave is caused by phase segregation between Ag and Sb under a constant electric current.

© 2025 Author(s). All article content, except where otherwise noted, is licensed under a Creative Commons Attribution-NonCommercial 4.0 International (CC BY-NC) license (<https://creativecommons.org/licenses/by-nc/4.0/>). <https://doi.org/10.1063/5.0259604>

I. INTRODUCTION

On many occasions, in nature and in life, specific spatiotemporal patterns are formed, accompanied by the dynamics of phase separation under thermodynamically open conditions, where energies and/or materials are continuously supplied and dissipated.¹⁻³ Such spatiotemporal systems can be classified as a new class of physical systems, different from the currently adopted theoretical models, such as reaction-diffusion in closed liquid systems^{4,5} or relaxation kinetics of phase segregation, such as nucleation-growth and spinodal decomposition.⁶⁻⁸ In general, life should be maintained as neither a closed reaction-diffusion system nor a monotonous relaxation system. A deeper understanding of the mechanisms of spatiotemporal pattern formation, in collaboration with the dynamic behavior of phase separation under thermodynamically open conditions, will contribute to unveiling the essence of life.

Electrochemical experiments are generally regarded as thermodynamically open systems. Previous experimental studies on electrochemical systems have reported the occurrence of temporal oscillations and the generation of stationary patterns,⁹⁻¹² along with some arguments about the possible effects of spatiotemporal instability. Interestingly, it has been found¹³⁻¹⁹ that the Ag and Sb

co-electrodeposition system, in which Ag and Sb atoms consistently accumulate on an electrode surface from a solution during electrodeposition, exhibits spatiotemporal behavior under the application of a stationary electrical current. Such a spatiotemporal pattern is regarded as generated under thermodynamically open conditions. It has been shown that various spatiotemporal patterns consisting of light and dark regions are formed on the electrode surface during electrodeposition depending on the experimental conditions. However, the mechanisms underlying these dynamical patterns have not yet been elucidated. Recently, the present authors discovered¹⁷ the occurrence of traveling waves on the electrode for the Ag and Sb co-electrodeposition system. In the present article, clear evidence on the generation of traveling waves is shown as in Fig. 1 for the complex labyrinthine structure. Intriguingly, the complex labyrinthine structure was formed on a solid electrode surface composed of metals. According to our static analysis of the chemical elements, the light and dark stripes in the pattern, which is observed optically, were assigned to regions rich in Ag and Sb, respectively.¹⁵ In our previous report on the time evolution of the stripe width, we argued that the phase separation of Ag and Sb in the electrodeposition system plays a fundamental role in the plausible pattern formation of the complex labyrinthine structure.^{16,18} In the present study, to

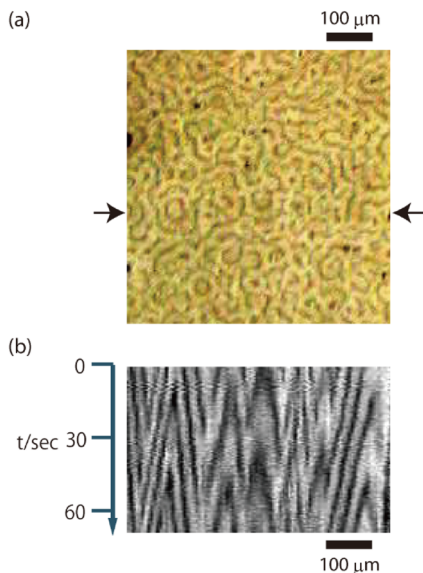


FIG. 1. (a) Optical microscope images of the complex labyrinthine structure. The applied current density is -9.75 mA/cm^2 . (b) Spatiotemporal diagram for the evolution of the stripe pattern along the line in between the two arrows depicted in image (a), indicating the generation of traveling waves migrating with nearly constant speed. The time series of color optical microscope images were converted to images of the gray scale to draw the spatio-temporal diagram in a clearer manner. Experimental conditions are described in the text, which are essentially the same as in our last paper.¹⁷

investigate the spatiotemporal structure based on the analysis of chemical elements in the electrodeposition system of Ag and Sb, *in situ* real-time element imaging through x-ray absorption analysis was carried out in an electrolyte solution under conditions where the complex labyrinthine structure emerges.

II. EXPERIMENTS

A. Preparation of an electrolyte solution to immerse the electrodes and an electrochemical machine to apply the constant current to the electrodes

An aqueous solution containing 0.26 M AgNO_3 , $0.27 \text{ M K}_4\text{Fe}(\text{CN})_6 \cdot 3\text{H}_2\text{O}$, and $0.27 \text{ M K}_2\text{CO}_3$ in distilled water was boiled for about 30 min to prepare the electrolyte solution used for the co-electrodeposition of Ag and Sb. After cooling, the Ag concentration was determined by titration. Next, $0.036 \text{ M K SbOC}_4\text{H}_4\text{O}_6 \cdot 3\text{H}_2\text{O}$ (potassium antimony tartrate), 1.5 M KSCN , and $0.21 \text{ M KNaC}_4\text{H}_4\text{O}_6 \cdot 4\text{H}_2\text{O}$ (potassium sodium tartrate) were added to the 0.15 M Ag aqueous solution. With this electrolyte solution, a complex labyrinthine structure appeared on the surface of the working electrode during electrodeposition within a range of current densities applied to the electrode (-11.8 – -9.7 mA/cm^2) in the constant-current mode [to maintain the constant current, the galvanostat mode was used in a potentiostat–galvanostat in Hokuto Denko (Tokyo, Japan), HA-151], as shown in the phase diagram of our previous study.¹⁴ The potential value at which the complex labyrinthine structure emerges under the constant current mode was in the range of -760 – -680 mV vs SHE .¹⁹

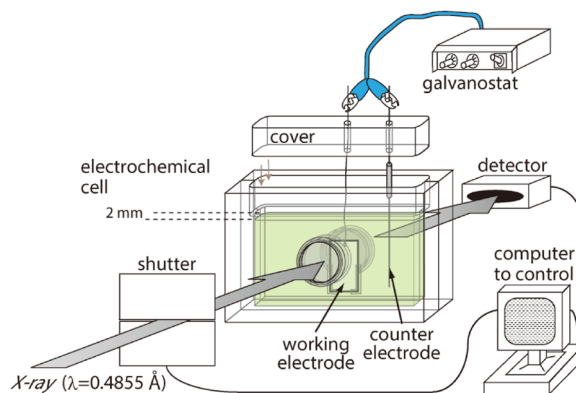


FIG. 2. Schematic for the experimental setup for *in situ* real-time element imaging analysis.

B. Fabrication of an electrochemical cell

As shown in Fig. 2, the electrochemical cell was prepared with acrylic plates, and the window (1 cm in diameter) through which the x-rays passed was fabricated using synthetic quartz to minimize the absorption caused by the experimental cell. While the radiation light passed through the electrochemical cell, the radiation x-rays were partly absorbed by the electrolyte–Ag solution and the electrode. The solution path of the cell was adapted to be 2 mm to reduce the absorption of the radiation x-rays by the electrolyte solution. The electrolyte solution was poured into a container of dimensions 8 cm (height) \times 13 cm (width) \times 2 mm (path). Two different electrodes were used; the working electrode, on which the pattern appeared, was placed on the inner side of the cell, while the counter electrode was placed 6 cm from the center of the cell. The counter electrode was a 1 mm (diameter) \times 5 cm (length) Ag wire. As a working electrode on which Ag and Sb were electrodeposited, an Au (111) thin film (200 nm in thickness) was placed on one side of a MICA insulating plate ($1 \times 2 \text{ cm}^2 \times \sim 100 \mu\text{m}$ in thickness). After the experiment, we visually confirmed the appearance of spatiotemporal patterns on the Au (111) surface upon which Ag and Sb were electrodeposited.

C. The *in situ* real-time elemental imaging using x-ray radiation

X-ray radiation was adapted for the *in situ* real-time elemental imaging (Fig. 2). Photons of 25.54 keV are absorbed by Ag (K absorption).²⁰ In the experiment, the radiation photons passed through the Au (111) thin film on the mica plate ($\sim 100 \mu\text{m}$ thickness) of the working electrode without absorption. A decrease in the transmission intensity caused by Ag absorption was detected for an illuminated area of $600 \mu\text{m} \times 1 \text{ mm}$. Therefore, if Ag atoms are electrodeposited on the working electrode composed of the Au (111) thin film and the mica plate, the transmission intensity of the x-ray passed through the electrode is decreased. The detector for the radiation light, a high-resolution x-ray indirect roentgenography camera with $0.5 \mu\text{m}$ spatial resolution and 0.2 s time resolution, was set on the exterior wall of the electrochemical cell to which the electrode was attached inside to detect the transmitted x-rays passing through the cell. For the observation of the time dependent change of the

x-ray absorbing pattern, repetitive opening of the shutter for the radiation x-ray (with a single photon energy of 25.54 keV) was performed by using a computer; the imaging of the Ag absorption of the radiation light for the illuminated area was taken every 20 s, while the exposure time was 500 ms. The obtained imaging data of the Ag absorption were subtracted from the imaging data of the blank observation control for Ag (25.50 keV) to reduce the noise.

III. RESULTS

Using a constant current density of -11.5 mA/cm^2 , which is applied to the electrodes, *in situ* real-time element imaging analysis for Ag was carried out by measuring the absorption of the x-ray specific for Ag. Figure 3 shows the time evolution of Ag absorption imaging. In the images, the light and dark colors show the low and high absorption of Ag x-ray radiation, respectively. However, because the background and tone curves for each image in Fig. 3 were modified to etch the shapes of the detected Ag absorption pattern, comparing the absolute values of the darkness between images from this figure was impossible. In the non-modified images, where only background noise was subtracted, a comparison of the darkness level was possible. The images became entirely darker with time because the film became thicker with the Ag electrodeposition (see Movie S1 for unmodified data). Figure 3 also shows that the two traveling light-colored stripes appeared first [see Figs. 3(a)–3(d)]; after the light-colored stripes appeared, the two traveling dark-colored stripes propagated, as seen in [Figs. 3(d) and 3(e)]. The widths of the light- and dark-colored stripes were $\sim 10 \mu\text{m}$. The stripe velocity was $\sim 1 \mu\text{m/s}$. (Five independent experiments under the same conditions were carried out, and in two out of the five experiments, traveling light and dark stripes were observed.)

After the two light-colored stripes traveled and collided, they disappeared [Figs. 3(d) and 3(e)]. This implies that the experiment exhibited the characteristics of a chemical reaction wave. In a chemical reaction wave, exemplified by the BZ reaction,⁴ annihilation occurs when two waves collide, and in these systems, the main elements of the stripes are uniformly distributed in space. The local chemically reacted compound forms a striped shape. In fact, the mechanism of the conventional chemical wave system explains the above-mentioned phenomenon, in which a specific element, whose atoms are uniformly dispersed, locally reacts and transforms into the activated reactant to form light-colored stripe shapes. In this case, the activated reactant of the specific element repelled the Ag^+ atoms and created a low Ag^+ concentration in the light-colored stripe. In the low Ag^+ concentration region, Sb^{3+} might be concentrated. When two light-colored stripes collided, the inhibitors following the light stripes caught up with the front colliding light stripes. Once this happened, inhibitors transformed the front activated reactants by forming light-colored stripes to the inactivated reactant, thereby ending the condition to repel the Ag^+ atoms (these inhibitors are chemical compounds containing the main element of the activated reactant, analogous to the BZ reaction). Therefore, the light-colored stripes disappeared during the collision. At present, what chemical specie(s) exhibited the effect of repelling Ag^+ needs to be clarified.

Following the propagation of light-colored stripes, the two dark-colored stripes (Ag^+ -rich region) propagated [Figs. 3(d)–3(f)]. The counter-propagating dark-colored stripes collided with each other, causing the dark-colored stripes to disappear. After their disappearance, many dark-colored round spots of $\sim 1 \mu\text{m}$ in size spontaneously emerged in the images [Figs. 3(g)–3(i')]. This suggests that Ag aggregates were generated in small domains after the collision

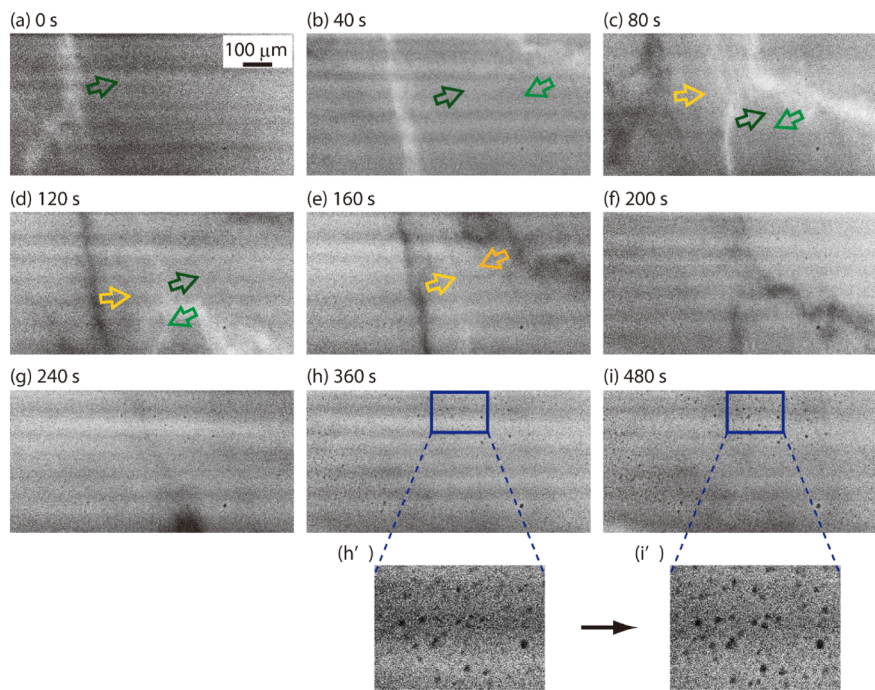


FIG. 3. Traveling waves obtained by the time-evolution of images in *in situ* real-time element imaging analysis for Ag. Image (a) was captured at 700 s after the start of electrodeposition. Light and dark-colored stripes indicate the areas of low and high Ag concentrations (low and high absorption of radiation light by Ag), respectively. [(h') and (i')] The enlarged images of the rectangular parts surrounded by blue lines in [(h) and (i)], respectively.

and the subsequent disappearance of the counter-propagating dark stripes.

IV. DISCUSSION

After the *in situ* real-time element analysis experiment, the surface of the electrode was observed using an optical microscope, and once it was removed from the solution, it was allowed to dry. In one local area of the electrode surface, the trace where the radiation was illuminated was rectangular ($\sim 600 \mu\text{m} \times 1 \text{mm}$ in size; see the [supplementary material](#)). In addition, many black domains of similar size to the dark-colored round spots observed in the Ag imaging were found on the uniform gray surface of the trace area. The black domains in the optical microscope imaging were in positions identical to the dark-colored round spots that appeared in the Ag imaging data [Figs. 3(g)–3(i)]. A comparison between the optical microscopy observations and the Ag imaging data reveals that the Ag^+ atoms existed as domains on the electrodeposited electrode surface. When Ag^+ -concentrated stripes, shown as dark-colored stripes, collided, the Ag^+ atoms did not disappear. In other words, this indicates that the dark-colored stripes exhibited a property that was different from that of a typical chemical wave, where they disappeared upon collision, and the main elements were uniformly distributed throughout the solution. The dark-colored stripes were formed by concentrated Ag^+ atoms, which were spatially separated from other areas, similar to phase separation.²¹ Therefore, the translational movement of the concentrated Ag^+ atom groups forming the striped shape supported the pattern-formation mechanism of phase separation, as suggested by the authors.

It is noted that the stripe shape was not similar to that of the complex labyrinthine structure (Fig. 1). On the other hand, the stripe width and stripe velocity were of the same order as those of the complex labyrinthine structure (~ 10 and $\sim 1 \mu\text{m/s}$, respectively). Therefore, after *in situ* real-time Ag imaging, we observed the electrode surface under dry conditions using an optical microscope. In this imaging, no complex labyrinthine pattern was observed in the area where the radiation was present, and the size of the black domains in the uniform gray film was found to be $\sim 1 \mu\text{m}$ in size. By contrast, at a position far from the radiation trace area, a complex labyrinthine structure was observed (as the applied current to the electrode was turned off, the shape of the complex labyrinthine structure was immobilized on the electrode surface). The results indicate that the radiation x-rays locally influenced the electrode surface condition. As a result, in the area where the radiation light was present, the complex labyrinthine structure was modified from the original shape, and the collision properties of the complex labyrinthine structure were not shown (in the original complex labyrinthine structure, the concentrated Ag^+ stripes were combined on their collision;¹⁶ see the spatiotemporal plot in Fig. 1). However, the experimental observation with x-rays reveals that Ag^+ waves indeed move within the electrode, spatially separating from other areas and forming a striped shape. This supports the mechanism by which phase separation of Ag^+ occurred in the film with Ag and Sb electrodeposited on the working electrode.

The conventional equation describing a traveling wave is as follows:

$$\partial\eta(r)/\partial t = L[-\varepsilon^2 \nabla^2 \eta - G(\eta)] + P(\eta), \quad (1)$$

where $\eta(r)$ is an order parameter (for example, a concentration of a chemical compound) at position r , and L and ε are constants. $G(\eta)$ indicates the concentration increases due to a chemical reaction, where $G(\eta) = -dW(\eta)/d\eta$ and $W(\eta)$ is a quartic function of η (first-order transition), and $W(\eta) \sim \eta^2(\eta^2 - a^2)$. $G(\eta)$ indicates, for example, the concentration increments due to the chemical reaction. $P(\eta)$ is the inflow and outflow of η in unit time and is a term of the non-equilibrium system. Equation (1) is called the reaction–diffusion equation²² and assumes the emergence of a traveling wave.

However, if the complex labyrinthine structure was driven by the phase separation of metals, the mechanism was phase separation in a nonequilibrium system. Because a constant current was applied, and the Ag and Sb atoms were constantly adsorbed to the electrode, a complex labyrinthine structure emerged and moved. In the case of phase separation in a nonequilibrium system, the equation is written as follows:

$$\partial\eta(r)/\partial t = L\nabla^2[-\varepsilon^2 \nabla^2 \eta - G(\eta)] + P(\eta). \quad (2)$$

The difference between Eqs. (1) and (2) is a notation of ∇^2 on the right side of Eq. (2). In Eq. (1), we have $-L[-\varepsilon^2 \nabla^2 \eta - G(\eta)]$, whereas, in Eq. (2), we have $L\nabla^2[-\varepsilon^2 \nabla^2 \eta - G(\eta)]$. Therefore, $G(\eta) = -dW(\eta)/d\eta$, where $W(\eta)$ is a term for internal energy and entropy (free energy) in the unit area and is also a quartic function of η . If $P(\eta)$ is absent in Eq. (2), the Cahn–Hilliard equation^{7,8} represents phase separation in a conserved system (relaxation system). Here, $\eta(r)$ is the Ag concentration. Because mass and charge transfers occur on the electrode, this system is considered thermodynamically open, and the term $P(\eta)$ should be considered. In the absence of $P(\eta)$, a traveling wave (one of the characteristics of the complex labyrinthine structure) does not appear. Therefore, for the complex labyrinthine structure, the traveling wave can appear with the addition of $P(\eta)$. T. Okuzono and T. Ohta discovered that a traveling wave appeared in a simulation under a phase separation system with the addition of $P(\eta)$ in terms of chemical reactions (non-conserved quantities).² However, in our previous attempt at numerical calculations, the constant-current mode operated on the electrode (the present system) added one condition, $\int \eta(r) dr = \text{Const}$ (global coupling to a conserved quantity), and is referred to as $P(\eta)$.¹⁸ Despite this, a traveling wave did not appear, which could be because the term $P(\eta)$ was used only in a conserved system. $P(\eta)$ might require the term representing the condition of the non-conserved system to create the traveling wave, similar to $P(\eta)$ being adapted as the chemical reaction term in Eq. (1). The emergence mechanism of the complex labyrinthine structure in the Ag and Sb co-electrodeposition system was expected to be similar to the framework adopting the reaction–diffusion system (the non-conserved system) in the phase separation system. To realize the traveling wave in the phase separation of a binary system, other researchers suggest nonreciprocal Cahn–Hilliard models breaking action–reaction symmetry.^{23–27} In the Ag and Sb co-electrodeposition system, it might be catalytic electroadsorption of one element (for example, it is electrodeposition of Ag^+ with high conductivity). It induces inbound flow of the other element (the local area with high conductivity also induces adsorption of Sb^{3+}). Afterward, outward repulsion of the adsorbed element occurs from the catalytic element (as the system favors the low consumption system, it might repel Sb^{3+} with the low conductivity from

the local area with high conductivity and retain the local area with high conductivity¹⁸).

Phase separation of molten metals in ordinary systems occurred at high temperatures, whereas the complex labyrinthine structure formed by the phase separation of Ag and Sb emerged at room temperature. The material comprising the complex labyrinthine structure might become a solid electrolyte. In a solid electrolyte material, the elemental atoms could move not only on the surficial liquid-phase but also through the solid layer in response to the applied voltage. Ag₂S is a typical solid electrolyte. In Ag₂S, Ag⁺ can move following an applied voltage at room temperature.²⁸ The Ag and S components of the above solid electrolyte were also included in the complex labyrinthine structure.¹⁵ This indicates that the material formed in the present system may have become a solid electrolyte. The difference between the present system and the Ag₂S system is the Sb inclusion. In the present system, Sb is one of the main components. In a previous study,²⁹ a composite of Ag, Sb, and S was used as a solid electrolyte. However, the characteristics of Ag, Sb, and S composites have rarely been investigated so far.

V. CONCLUSIONS

The propagation of the Ag stripe was successfully observed at room temperature through an *in situ* real-time elemental analysis. This observation implied that a stripe was formed by the phase separation of Ag in a nonequilibrium system. However, the stripe shape was different from the conformation of the complex labyrinthine structure because of its influence on radiation incidence. An improvement in the experimental conditions will be our future assignment. Currently, the common theoretical framework for traveling waves under dissipative conditions is a reaction-diffusion system. In contrast, this study found that the phase-segregated band exhibited the characteristics of a traveling wave with global feedback under thermodynamically open conditions. The observed phenomenon of spatiotemporal pattern formation in the present study is accompanied by phase-segregation under constant electric current conditions, being much different from the current reports on the generation of traveling waves in reaction-diffusion systems. A similar phenomenon was expected in many other systems. In fact, spatiotemporal patterns have recently been discovered under several other metal alloys, such as Co-In, in electrodeposition systems.³⁰⁻³⁶

SUPPLEMENTARY MATERIAL

The [supplementary material](#) provides an image obtained with an optical microscope that shows the electrode surface after *in situ* real-time Ag imaging.

ACKNOWLEDGMENTS

Synchrotron radiation experiments were performed at BL20XU at SPring-8 with the approval of the Japan Synchrotron Radiation Research Institute (JASRI) (Proposal No. 2008A1089). We appreciate the technical support of Yoshio Suzuki and Akihisa Takeuchi of the JASRI for the automatic control measurement. We are grateful for the tremendous help from Hiroshi Tamura and the members

of the Machine Shop Technical Staff in the Division of Physics and Astronomy, Graduate School of Science, Kyoto University, in fabricating the electrochemical cell for the experiment. This work was supported by JSPS KAKENHI (Grant No. JP24K06908).

AUTHOR DECLARATIONS

Conflict of Interest

The authors declare the following financial interests/personal relationships, which may be considered potential competing interests: Our reports financial support was provided by the Japan Society for the Promotion of Science.

Author Contributions

Yuko Nagamine: Conceptualization (equal); Data curation (equal); Formal analysis (equal); Funding acquisition (equal); Investigation (equal); Methodology (equal); Resources (equal); Software (equal); Validation (equal); Visualization (equal); Writing – original draft (equal); Writing – review & editing (equal). **Kenichi Yoshikawa:** Data curation (supporting); Formal analysis (supporting); Funding acquisition (equal); Investigation (supporting); Methodology (supporting); Resources (supporting); Supervision (lead); Validation (equal); Writing – original draft (equal).

DATA AVAILABILITY

The data that support the findings of the study are available within the article and its [supplementary material](#).

REFERENCES

- 1 M. C. Cross and P. C. Hohenberg, *Rev. Mod. Phys.* **65**, 851 (1993).
- 2 T. Okuzono and T. Ohta, *Phys. Rev. E* **67**, 056211 (2003).
- 3 M. Hildebrand, A. S. Mikhailov, and G. Ertl, *Phys. Rev. Lett.* **81**, 2602 (1998).
- 4 A. N. Zaikin and A. M. Zhabotinsky, *Nature* **225**, 535 (1970).
- 5 S. Kondo and T. Miura, *Science* **329**, 1616 (2010).
- 6 Y. Oono and S. Puri, *Phys. Rev. A* **38**, 434 (1988).
- 7 J. W. Cahn and J. E. Hilliard, *J. Chem. Phys.* **28**, 258 (1958).
- 8 J. W. Cahn and J. E. Hilliard, *J. Chem. Phys.* **31**, 688 (1959).
- 9 K. Krischer, N. Mazouz, and P. Grauel, *Angew. Chem., Int. Ed.* **40**, 850 (2001).
- 10 M. T. M. Koper, *Adv. Chem. Phys.* **92**, 161 (1996).
- 11 I. Golvano-Escobar *et al.*, *Sci. Rep.* **6**, 30398 (2016).
- 12 A. Lahiri *et al.*, *Sci. Adv.* **4**, eaau9663 (2018).
- 13 I. Krastev and M. T. M. Koper, *Physica A* **213**, 199 (1995).
- 14 Y. Nagamine and M. Hara, *Physica A* **327**, 249 (2003).
- 15 Y. Nagamine and M. Hara, *Phys. Rev. E* **72**, 016201 (2005).
- 16 Y. Nagamine and M. Hara, *Surf. Sci.* **601**, 803 (2007).
- 17 Y. Nagamine and K. Yoshikawa, *Chaos* **20**, 023117 (2010).
- 18 Y. Nagamine, *Physica A* **604**, 127925 (2022).
- 19 Y. Nagamine, N. Kurono, and M. Hara, *Thin Solid Films* **460**, 87 (2004).
- 20 J. G. Speight, *Lange's Handbook of Chemistry* (McGraw-Hill, New York, 2005), p. 3.134.
- 21 K. Binder, in *Material Science and Technology: Phase Transformations in Materials*, edited by P. Haasen (VCH, Weinham, 1991), Vol. 5, p. 409.
- 22 A. Saul and K. Showalter, in *Oscillations and Traveling Waves in Chemical Systems*, edited by J. Field, M. Burger (New York, Wiley, 1985), Chap. 11.
- 23 S. Saha, J. Agudo-Canalejo, and R. Golestanian, *Phys. Rev. X* **10**, 041009 (2020).

- ²⁴T. Frohoff-Hülsmann, U. Thiele, and L. M. Pismen, *Philos. Trans. R. Soc. A* **381**, 20220087 (2023).
- ²⁵F. Brauns and M. C. Marchetti, *Phys. Rev. X* **14**, 021014 (2024).
- ²⁶Z. You, A. Baskaran, and M. C. Marchetti, *PNAS* **117**, 19767 (2020).
- ²⁷N. Rana and R. Golestanian, *Phys. Rev. Lett.* **133**, 078301 (2024).
- ²⁸K. Terabe, T. Hasegawa, T. Nakayama, and M. Aono, *Nature* **433**, 47 (2005).
- ²⁹*Fast Ion Transport in Solids*, edited by W. van Gool (North-Holland Publishing, Co.; American Elsevier Publishing, Co., Amsterdam-London; NewYork, 1972), p. 280 Table V.
- ³⁰D. Lacitignola, I. Sgura, B. B. T. Dobrovolska, and I. Krastev, *Commun. Nonlinear Sci. Numer. Simulat.* **79**, 1049030 (2019).
- ³¹B. Bozzini, P. Bocchetta, A. Gianoncelli, C. Mele, and M. Kiskinova, *ChemElectroChem* **2**, 1541 (2015).
- ³²Y. Sun and G. Zangari, *J. Electrochem. Soc.* **166**(8), D339 (2019).
- ³³J. Yang, Y. Jia, Q. Gao, C. Pan, Y. Zhao, W. Bi, and G. Xie, *J. Solid State Electrochem.* **19**, 3265 (2015).
- ³⁴R. Fernández Mateo, V. Calero, H. Morgan, P. García-Sánchez, and A. Ramos, *Phys. Rev. E* **108**, 015104 (2023).
- ³⁵O. Lev, M. Sheintuch, L. M. Pisemen, and Ch. Yarnitzky, *Nature* **336**, 458 (1988).
- ³⁶B. Bozzini, D. Lacitignola, C. Mele, and I. Sgura, *Note Mat.* **32**, 7 (2012).